A Direct Torque Controlled Induction Motor with Variable Hysteresis Band

Kanungo Barada Mohanty
Electrical Engineering Department, National Institute of Technology, Rourkela, India

***Abstract*—An improved direct torque controlled induction motor drive is reported in this paper. It is established that the conventional direct torque controlled drive has more torque and flux ripples in steady state, which result in poor torque response, acoustic noise and incorrect speed estimations. Hysteresis controllers also make the switching frequency of voltage source inverter a variable quantity. A strategy of variable duty ratio control scheme is proposed to increase switching frequency, and adjust the width of hysteresis bands according to the switching frequency. This technique minimizes torque and current ripples, improves torque response, and reduces switching losses in spite of its simplicity. Simulation results establish the improved performance of the proposed direct torque control method compared to conventional methods.**

Keywords—Direct Torque Control, Hysteresis controllers, Switching Frequency, Torque Ripple, Induction Motor Drive

NOMENCLATURE

$\overline{v}_s$, $\overline{i}_s$	stator voltage vector and current vector
$\overline{\psi}_s$, $\overline{\psi}_r$	stator and rotor flux linkage vectors
$\overline{\psi}_{s,ref}$	reference stator flux linkage vector
$\overline{v}_{s,k}$	stator voltage vector in k-th sector of flux plane
$\Delta\overline{\psi}_s$	change in stator flux linkage vector in time Δt
T_e	developed torque of machine
T_{ref}	reference torque
ΔT	half the width of torque hysteresis band
θ_{sr}	angle between stator and rotor flux vectors
$d\psi$, dT_e	flux and torque error status
V_{dc}	dc link voltage input to inverter
R_s	stator resistance per phase
L_s ,L_r, L_m	stator (self), rotor (self) and mutual inductances
σ	stator flux leakage coefficient
P	number of poles

I. INTRODUCTION

Many adjustable speed drive applications require instantaneous electromagnetic torque control, instead of precise, closed loop speed control. The advantages of torque control in this type of application include greatly improved transient response, avoidance of over-current trips, and the elimination of load dependent controller parameters. An example of an application where torque is to be controlled, without precise speed control, is traction drives for electric vehicles.

There are basically two types of instantaneous torque controlled a.c. drives used for high performance applications: vector controlled, and direct torque controlled drives. Vector controlled drives [1], were introduced more than 30 years ago. They have achieved a high degree of maturity and have become increasingly popular in a wide range of applications. However, complexity of coordinate transformation, inclusion of shaft encoder, and parameter dependency are well known disadvantages of vector controlled drives [1]. To overcome these problems, direct torque control (DTC) [2], or direct self control (DSC) [3], [4] technique was introduced. In this method the inverter is switched so as to keep stator flux and torque within the limits of two hysteresis bands. This method allows a decoupled control of flux and torque without the need of coordinate transformation, PWM pulse generation and current regulation but results in a variable switching frequency. At steady state current, flux and torque pulsates, which result in inaccurate flux and speed estimation, and increased acoustical noise.

Several solutions with improved DTC are presented in the literature. To improve torque and flux response and reduce inverter switching frequency of a high power drive, two inverters with DTC is implemented in [5]. In [6,7], techniques have been presented which allow constant switching frequency operation. Over a fixed switching period, inverter switching pattern or duty cycle is calculated in [6] directly in order to control the torque and flux in a deadbeat fashion. Reduction of current and torque ripple is obtained in [7] by calculating the required variation of stator flux vector, and exactly compensating the flux and torque errors. To apply this technique, the control system should be capable of generating any voltage vector at each sampling period. This concept is applied in [5] to generate a number of voltage vectors higher than that used in basic DTC, by using a double three phase inverter. Direct torque and flux control (DTFC) based on space vector modulated (SVM) inverter for sensorless induction motor drive is implemented in [8]. Constant and controllable switching frequency is achieved, and steady state torque ripple is reduced. Discrete space vector modulation (DSVM) technique is used in [9] to increase the number of voltage vectors. Voltage vectors are selected in [9] from switching tables according to rotor speed, flux error and torque error. This reduces flux and torque ripples, and current distortion. In [10], a comparative study of classical DTC, space vector modulated (SVM) DTC and discrete space vector modulated (DSVM) DTC is done with emphasis on stator current distortion and torque ripple.

In this paper, the principle of direct torque and flux control is discussed in section II. The improved DTC technique is presented in section III. The strategy for

978-0-7695-3593-7/09 $25.00 © 2009 IEEE
DOI 10.1109/UKSIM.2009.24

IEEE computer society

Authorized licensed use limited to: NATIONAL INSTITUTE OF TECHNOLOGY ROURKELA. Downloaded on September 17, 2009 at 07:03 from IEEE Xplore. Restrictions apply.

adjusting the width of hysteresis band to reduce torque and flux ripples is also reported in section III. Test results are presented in section IV.

II. DIRECT TORQUE AND FLUX CONTROL

The scheme of conventional direct torque controlled induction motor drive is shown in Fig. 1. It consists of a pair of hysteresis comparator, torque and flux estimators, voltage vector selector and a voltage source inverter.

The schematic diagram of 3-phase voltage source inverter is shown in Fig. 2. It has eight possible voltage space vectors, as shown in Fig. 3, according to the combination of the switching modes: k = [S_a S_b S_c] where each of S_a, S_b, S_c takes the value 1 or 0 independent of others. There are six active voltage vectors: $\bar{v}_{s,1}$ to $\bar{v}_{s,6}$ and two zero voltage vectors: $\bar{v}_{s,0}$, $\bar{v}_{s,7}$ corresponding to [0 0 0] and [1 1 1], respectively. It can be shown that the voltage vector is given by (1).

$$\bar{v}_{s,k} = \frac{2}{3} V_{dc} \left[S_a + S_b \, e^{j.2\pi/3} + S_c \, e^{j.4\pi/3} \right] \qquad (1)$$

DTC performs separate control of the stator flux and torque, which is also known as decoupled control. Direct flux control and direct torque control are discussed in the following sections.

A. Direct Flux Control

A dynamic model of the machine is considered to design and simulate the direct torque control technique. The machine model in stator reference frame [1], is used for simulation. The stator flux linkage vector is given as [1],

$$\bar{\psi}_s = \int (\bar{v}_s - R_s \bar{i}_s) \cdot dt \qquad (2)$$

Neglecting the voltage drop in stator resistance, the flux change over a small period of time can be written as

$$\Delta \bar{\psi}_s = \bar{v}_s \cdot \Delta t \qquad (3)$$

In (3), $\bar{v}_s$ is the voltage vector, which may occupy any of the eight space positions as shown in Fig. 3.

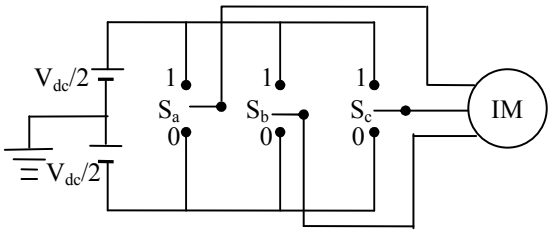

Figure 2. Schematic diagram of voltage source inverter

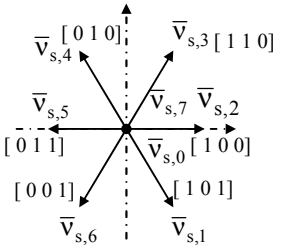

Figure 3. Voltage space vectors

The magnitude and orientation of the stator flux must be known in order to directly control the stator flux by selecting appropriate voltage vector. The stator flux plane is divided into six sectors as shown in Fig. 4. Each sector has a different set of voltage vectors to increase (voltage vector highlighted in gray) or decrease (voltage vector highlighted in black) the stator flux as illustrated in Fig. 4. The stator flux is forced to follow the reference value within a hysteresis band by using a 2-level hysteresis comparator. If the stator flux lies in sector k, then the voltage vector $\bar{v}_{s,k+1}$ is selected to increase the stator flux, and $\bar{v}_{s,k+2}$ selected to decrease the stator flux.

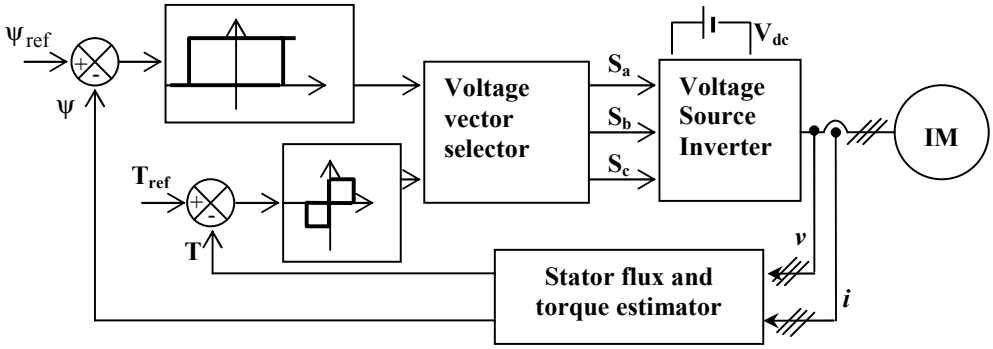

Figure 1. Schematic diagram of direct torque controlled induction motor drive

Authorized licensed use limited to: NATIONAL INSTITUTE OF TECHNOLOGY ROURKELA. Downloaded on September 17, 2009 at 07:03 from IEEE Xplore. Restrictions apply.

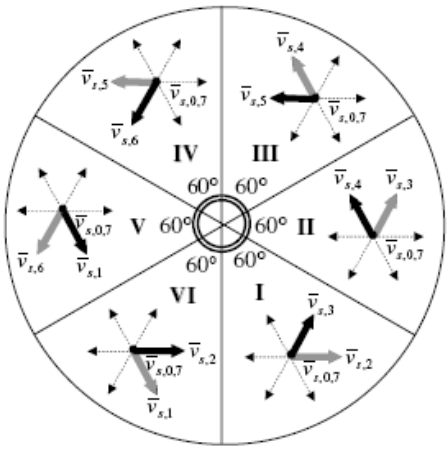

Figure 4. Control of voltage space vectors in six sectors of flux plane

The radial voltage vectors $\overline{v}_{s,k}$ and $\overline{v}_{s,k+3}$, which can be used to quickly affect the flux, are generally avoided. The estimated stator flux error is fed to the hysteresis comparator as shown in Fig. 5, which produces the flux error status $d\psi$. It can be either 1 or 0. Typical waveforms of stator flux, stator flux error and stator flux error status are shown in Fig. 6.

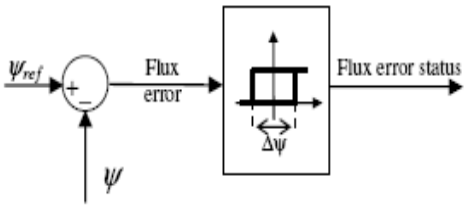

Figure 5. Block diagram of the stator flux hysteresis comparator

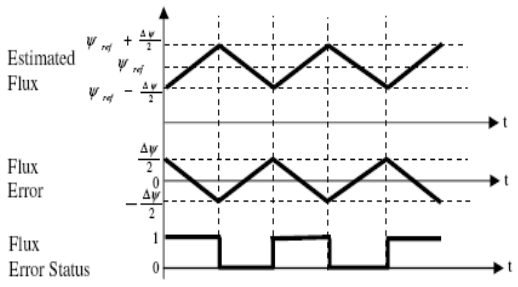

Figure 6. Waveforms of stator flux, flux error and flux error status

If stator flux is to be increased $d\psi = 1$, and if stator flux is to be decreased $d\psi = 0$.

$$d\psi = 1 \text{ if } |\overline{\psi}_s| \le |\overline{\psi}_{s,ref}| - |\Delta\psi_s| \quad (4)$$

$$d\psi = 0 \text{ if } |\overline{\psi}_s| \ge |\overline{\psi}_{s,ref}| + |\Delta\psi_s| \quad (5)$$

The performance of the control system is directly dependent on the estimation of stator flux and torque. Stator flux is estimated using the voltage model, as in (2).

B. Direct Torque Control

The instantaneous torque in terms of stator and rotor flux linkages is given by (6).

$$T_e = \frac{3}{2}\frac{L_m}{\sigma L_s L_r}\overline{\psi}_s \times \overline{\psi}_r = \frac{3}{2}\frac{L_m}{\sigma L_s L_r}\psi_s \psi_r \sin\theta_{sr} \quad (6)$$

In order to obtain instantaneous torque control, it is necessary to vary θ_{sr} quickly. Variation of θ_{sr} and electromagnetic torque with the application of different voltage vectors are given in Table I. Two assumptions are motor rotates in counterclockwise rotation, and load torque remains constant. It can be summarized that, the stator flux which lies in sector k, plays an important role in controlling θ_{sr} by applying an appropriate voltage vector as tabulated in Table I.

TABLE I. VARIATION OF θ_{sr} AND T_E WITH DIFFERENT VOLTAGE VECTORS

Voltage vector	Effect on stator flux	θ_{sr}, and T_e
Active forward ($\overline{v}_{s,k+1}$ and $\overline{v}_{s,k+2}$)	Stator flux advances forward	Increase
Zero ($\overline{v}_{s,0}$ and $\overline{v}_{s,7}$)	Stator flux weakens only due to stator resistance drop	Decrease
Radial ($\overline{v}_{s,k}$ and $\overline{v}_{s,k+3}$)	Stator flux magnitude increases or reduces rapidly	Decrease
Reverse active ($\overline{v}_{s,k-1}$ and $\overline{v}_{s,k-2}$)	Stator flux rotates in reverse direction	Decrease rapidly

In DTC, the torque is controlled within its hysteresis band similar to the stator flux. Three-level hysteresis controller as shown in Fig. 7 is employed because the machine may operate in motoring mode as well as braking mode as shown in Fig. 8. Waveforms of the torque, torque error, speed and torque error status are shown in Fig. 8. Torque error status, dT_e=1, −1 or 0, if the torque is to be increased, decreased or not to be changed, respectively.

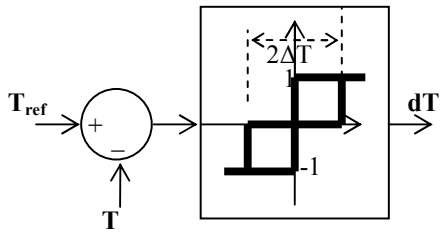

Figure 7. Block diagram of 3-level torque hysteresis comparator

Authorized licensed use limited to: NATIONAL INSTITUTE OF TECHNOLOGY ROURKELA. Downloaded on September 17, 2009 at 07:03 from IEEE Xplore. Restrictions apply.

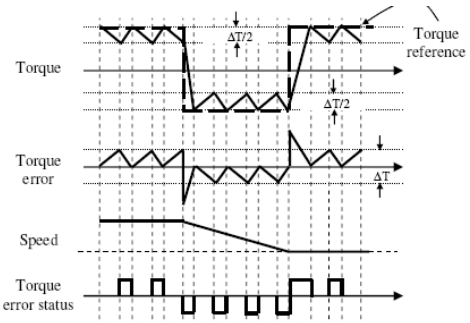

Figure 8. Waveforms of torque, torque error and torque error status

When a negative reference torque is applied, motor enters to braking mode, and the torque error status alternates between –1 and 0. When the reference torque is positive, the torque error status switches between 1 and 0, indicating motoring mode operation. The developed torque is estimated from the stator flux and the stator current space vectors, using (7).

$$T_e = \frac{3}{2}\frac{P}{2}\bar{\psi}_s \times \bar{i}_s \qquad (7)$$

III. CONTROL TECHNIQUE

A. Voltage Vector Selection

Due to the decoupled control of torque and stator flux in DTC, a high performance torque control can be established. If stator flux lies in sector k with motor rotating in counter clockwise, active voltage vector $\bar{v}_{s,k+1}$ is used to increase both stator flux and torque, where as $\bar{v}_{s,k+2}$ is selected to increase torque but decrease stator flux. The two zero voltage vectors ($\bar{v}_{s,0}$ and $\bar{v}_{s,7}$) are used to reduce the torque and freeze the stator flux. In this case stator flux weakens only due to stator resistance drop. In forward braking mode, reverse voltage vector $\bar{v}_{s,k-2}$ is used to decrease both torque and flux, where as $\bar{v}_{s,k-1}$ is selected to reduce the torque and increase the flux. The optimum selection of switching vectors in all sectors of stator flux plane is tabulated in Table II for counterclockwise rotation, and in Table III for clockwise rotation.

TABLE II. VOLTAGE VECTOR SELECTION FOR COUNTERCLOCKWISE ROTATION

Flux error stats	Torq error status	Sector 1	Sector 2	Sector 3	Sector 4	Sector 5	Sector 6
0	1	110	010	011	001	101	100
	0	111	000	111	000	111	000
	-1	011	001	101	100	110	010
1	1	100	110	010	011	001	101
	0	000	111	000	111	000	111
	-1	001	101	100	110	010	011

TABLE III. VOLTAGE VECTOR SELECTION FOR CLOCKWISE ROTATION

Flux error stats	Torq error status	Sector 1	Sector 2	Sector 3	Sector 4	Sector 5	Sector 6
0	1	011	001	101	100	110	010
	0	111	000	111	000	111	000
	-1	110	010	011	001	101	100
1	1	001	101	100	110	010	011
	0	000	111	000	111	000	111
	-1	100	110	010	011	001	101

B. Switching Frequency

The variable switching frequency may produce significant acoustic noise of variable intensity, a non-uniform distribution of switching losses for each semiconductor switch in the power inverter, and currents that have nondeterministic harmonic content. Many techniques are proposed and implemented to produce constant switching frequency for DTC. Basically, they can be divided into hysteresis based, and non-hysteresis based solutions. A variable hysteresis band comparator is proposed in this paper, where the band is adjusted according to the switching frequency.

C. Torque Ripple

With a larger sampling time, the possibility of torque overshoot and undershoot is higher. By reducing the sampling period, a better torque trajectory is obtained. Switching frequency is increased by changing the duty ratio of the selected voltage vector during each switching period according to the magnitude of the torque error and position of the stator flux. Here a zero voltage vector is chosen to reduce the torque.

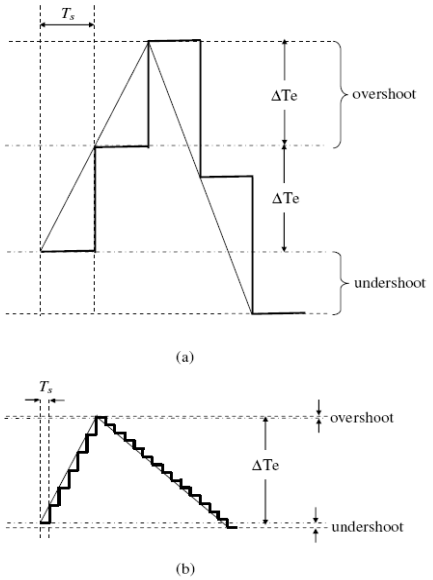

Figure 9. Two trajectories of torque with (a) large sampling time, (b) small sampling time

Authorized licensed use limited to: NATIONAL INSTITUTE OF TECHNOLOGY ROURKELA. Downloaded on September 17, 2009 at 07:03 from IEEE Xplore. Restrictions apply.

IV. TEST RESULTS

For the simulation, the induction motor whose specifications and parameters are given in Table-IV is used. The reference flux linkage is taken as 1V.s and starting torque is limited to 15 N-m.

The SIMULINK block diagram for the proposed drive system is shown in Fig. 10. The model is run for typical conditions of reference speed and applied torque values. The simulation results of the starting transients for the DTC drive at no load condition are shown in Fig. 11. The simulation results of the DTC drive for load variations are shown in Fig. 12. The hexagonal flux plot of stator flux linkage is shown in Fig. 13. Fig. 14 shows the locus diagram of stator flux linkage vector with load variation. Time variations of flux and torque are shown in Fig. 15 and Fig. 16, respectively. Fig. 17 and Fig. 18 show the time variation of q-axis stator flux and d-axis stator flux, respectively.

TABLE IV. SPECIFICATION AND PARAMETERS OF THE INDUCTION MOTOR

Specifications	1.5kW, 1440 r.p.m., 4 pole, 3 phase, 50Hz
Parameters	Nominal values
R_s	7.83
R_r	7.55
L_s	0.4751H
L_r	0.4751H
L_m	0.4535H
J	0.06 Kg· m^2
B	0.01 N· m/rad/s

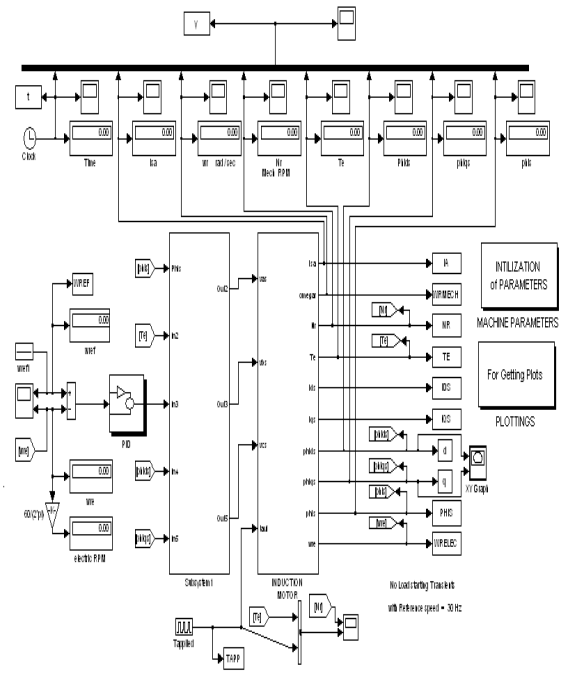

Figure 10. SIMULINK block diagram of the drive system

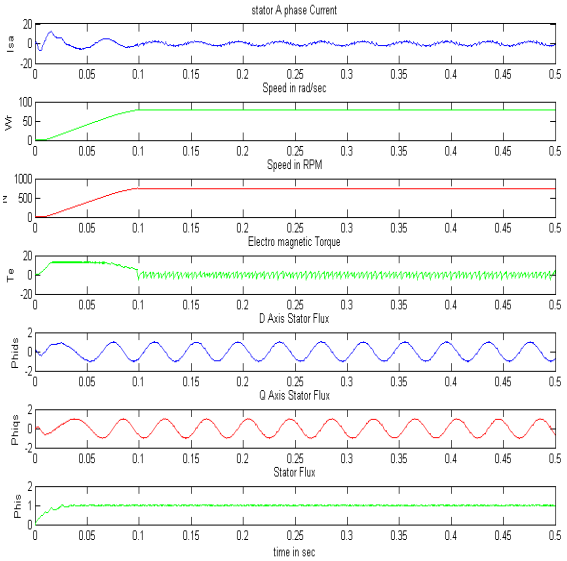

Figure 11. No-load starting transients

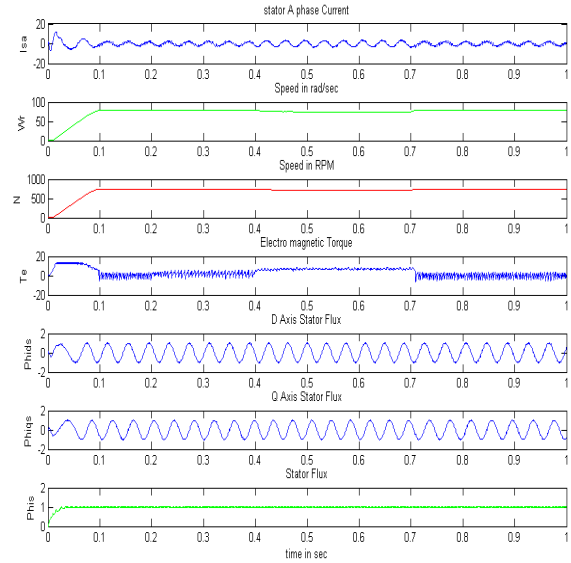

Figure 12. Starting transients with load variations

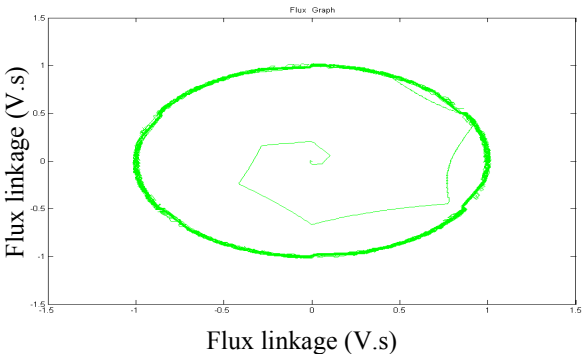

Figure 13. Hexagonal plot of stator flux linkage vector tip at no load

Authorized licensed use limited to: NATIONAL INSTITUTE OF TECHNOLOGY ROURKELA. Downloaded on September 17, 2009 at 07:03 from IEEE Xplore. Restrictions apply.

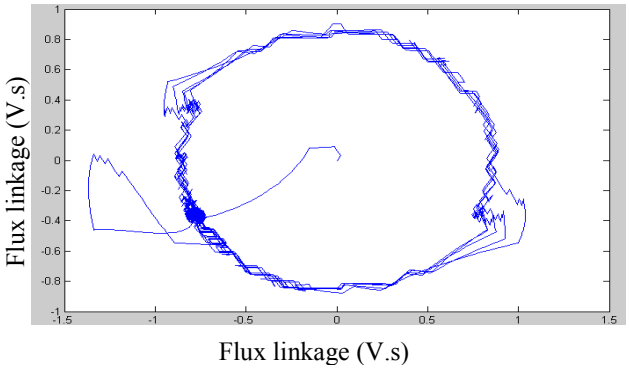

Figure 14. Locus of tip of stator flux linkage vector with load

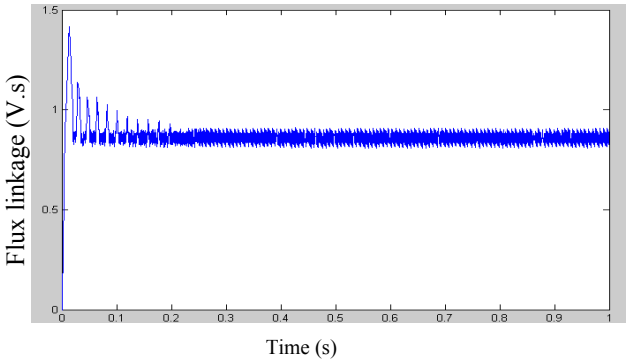

Figure 15. Flux linkage versus time

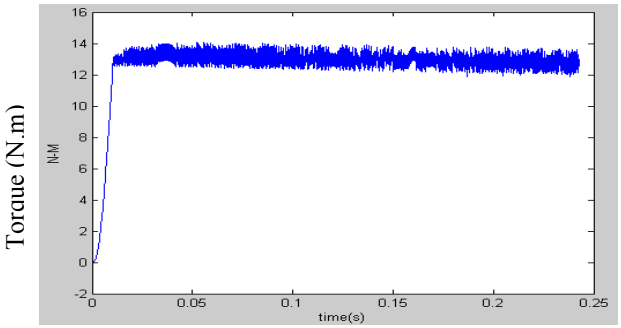

Figure 16. Torque versus time

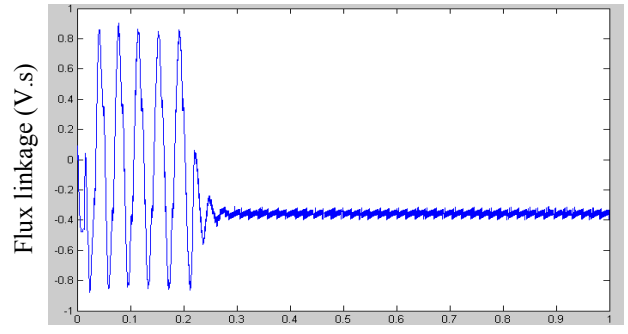

Figure 17. q-axis flux linkage versus time

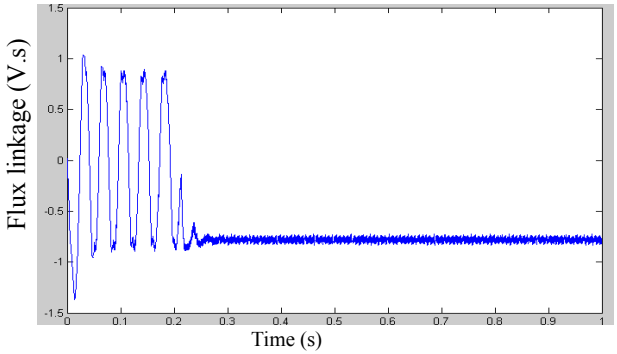

Figure 18. d-axis flux linkage versus time

V. CONCLUSIONS

The conventional direct torque control (DTC) strategy with fixed hysteresis band is simpler to implement than vector control, but it has high torque ripple and poor torque response. The proposed scheme uses a variable hysteresis band comparator, where the band is adjusted according to the switching frequency. Switching frequency is also increased significantly by varying the duty ratio of the selected voltage vector according to the magnitude of the torque error and position of the stator flux. Simulation results establish that the proposed technique has improved the torque response, and reduced the torque ripple. This DTC method also allows the decoupled control of torque and stator flux. So, a better drive performance is achieved.

REFERENCES

[1] P. Vas, Sensorless Vector and Direct torque control, Oxford University Press, 1998.

[2] I. Takahashi and T. Noguchi, A new quick response and high efficiency control strategy of an induction motor, IEEE Trans. Ind. Appl., vol. 22, no. 5, pp. 820-827, 1986.

[3] M. Depenbrock, Direct self control (DSC) of inverter-fed induction machines, IEEE Trans. Power Electronics, vol. 3, no. 4, pp. 420-429, 1988.

[4] U. Badder and M. Depenbrock, Direct self control (DSC) of inverter-fed induction machines: A basic for speed control without speed measurement, IEEE Trans. Ind. Appl., vol. 28, no. 3, pp. 581-588, 1992.

[5] I. Takahashi and Y. Ohmori, High-performance direct torque control of induction motor, IEEE Trans. Ind. Appl., vol. 25, no. 2, pp. 257-264, 1989.

[6] T. G. Habetler, F. Profumo, M. Pastorelli, and L. M. Tolbert, Direct torque control of induction machines using space vector modulation, IEEE Trans. Ind. Appl., vol. 28, no. 5, pp. 1045-1053, 1992.

[7] D. Casadei, G. Sera, and A. Tani, Stator flux vector control for high performance induction motor drives using space vector modulation, Electromotion, vol. 2, no. 2, pp. 79-86.

[8] C. Lascu, I. Boldea, and F. Blaabjerg, A modified direct torque control for induction motor sensorless drive, IEEE Trans. Industry Applications, vol. 36, no. 1, pp. 122-130, 2000.

[9] D. Casadei, G. Sera, and A. Tani, Implementation of a direct torque control algorithm for induction motors based on discrete space vector modulation, IEEE Trans. Power Electronics, vol.15, no.4, pp. 769-777, 2000.

[10] P. Marino, M. D'Incecco and N. Visciano, A comparison of direct torque control methodologies for induction motor, Procc. IEEE Porto Power Tech Conference, Portugal, Sept. 2001.

Authorized licensed use limited to: NATIONAL INSTITUTE OF TECHNOLOGY ROURKELA. Downloaded on September 17, 2009 at 07:03 from IEEE Xplore. Restrictions apply.